Phys. Status Solidi A **207**, No. 5, 1070–1073 (2010) / **DOI** 10.1002/pssa.200983113

physica status solidi a
www.pss-a.com
applications and materials science

The role of InGaN interlayers on the microstructure of InN epilayers grown via metal organic vapour phase epitaxy

Abdul Kadir[1], Tapas Ganguli[2], M. R. Gokhale[1], A. P. Shah[1], and Arnab Bhattacharya[*,1]

[1] Tata Institute of Fundamental Research, Homi Bhabha Road, Mumbai 400005, India
[2] Raja Ramanna Centre for Advanced Technology, Indore 425013, India

Received 8 September 2009, revised 27 November 2009, accepted 1 December 2009
Published online 9 March 2010

Keywords InN films, MOVPE, InGaN interlayers, microstructure, dislocations

[*] Corresponding author: e-mail arnab@tifr.res.in, Phone: +91 22 2278 2517, Fax: +91 22 2280 4610

A detailed study on the influence of an InGaN interlayer between the GaN buffer and InN epilayer on the microstructural properties of the InN layer is reported. Using high-resolution X-ray diffraction measurements the mosaicity of MOVPE grown InN epilayers deposited directly on c-plane sapphire, on GaN buffer layers, and on different InGaN interlayers have been compared. Generally the angle of tilt and hence the screw dislocation density in the InN epilayers can be controlled by growth conditions, while the angle of twist, corresponding to the edge dislocation density is usually weakly dependent on growth conditions. However, for a given layer thickness the edge dislocation density can be significantly reduced by the insertion of an InGaN interlayer.

1 Introduction The synthesis of high quality InN epilayers is one of the most challenging among the Group III-Nitride semiconductors. Apart from the large lattice mismatch with the commonly used sapphire substrates, growth of InN by MOVPE is particularly difficult because of the narrow growth temperature window and the use of relatively high (>10,000) V/III ratios [1]. The microstructures of the deposited films are hence very sensitive to the growth conditions. We have earlier reported a comprehensive investigation of the growth parameter space for the epitaxy of InN in a close-coupled showerhead reactor system [2] and also presented a detailed analysis of the influence of growth parameters on the inbuilt strain [3] and microstructure of the epilayers [4]. Those InN epilayers were deposited on GaN buffer layers or directly on c-plane sapphire substrates. However, the lattice mismatch between InN and GaN or sapphire is very large which results in a high dislocation density with the epilayer being composed of a large number of mosaic blocks with in-plane (twist) and out-of-plane (tilt) misorientation with respect to each other. The lattice mismatch between InN and GaN is 11% [1] and the mismatch between InN and sapphire is −25 or 29% (depending on the orientation) [5]. The use of compositionally graded layers or growth on a material of intermediate lattice constant has been a standard route to improve material quality in a range of material systems like SiGe [6], InGaAs/GaAs [6, 7], and GaAs/Si [8]. For the Group III-Nitrides, the insertion of low-temperature grown interlayers for dislocation reduction is common for the growth of GaN and AlGaN layers [9]. However, while there are reports which describe the growth of thin InN quantum wells embedded within high indium concentration $In_xGa_{1-x}N$ barriers [10–12], there is very little reported data [13] on the role of an InGaN intermediate layer for the growth of thicker InN layers. For example, Che et al. [10, 12] reported the growth of InN/InGaN (3–16 nm/9 nm) multi-quantum wells (MQWs) on GaN underlayer and also studied the effect of the InN well thickness on the photoluminescence (PL) peak position. Ohashi et al. [11] also showed the effect of QW thickness on PL emission wavelength in InN/$In_{0.75}Ga_{0.25}N$ MQWs. These results are on samples grown by molecular beam epitaxy. Recently, Hartono et al. [13] attempted MOVPE growth of InN on GaN using a thin InGaN interlayer and reported pyramidal island growth for the InN rather than smooth InN layers. However, they did not show any PL emission from the InN layer. None of these groups have studied the influence of the InGaN on the crystallinity and microstructure of InN epilayers. Here we discuss the role of the InGaN interlayer on

the mosaicity of InN epilayers using high resolution X-ray diffraction (HRXRD).

2 Experimental All the InN epilayers studied in this work were grown on on 2-inch c-plane sapphire substrates via MOVPE in a 3×2 inch close-coupled showerhead reactor system (Thomas Swan) using trimethylindium (TMIn) and ammonia (NH_3) precursors with nitrogen as the carrier gas. The deposition parameters were optimized for best crystalline quality of InN epilayers which was reported in a prior work [2]. Using these optimized deposition parameters for the InN layer (temperature = 530 °C, reactor pressure = 500 Torr or 0.66×10^5 Pa, V/III ratio = 18,700, and growth rate 0.2 μm/h) a series of 0.2 μm thick InN epilayers on InGaN were grown where the temperature, indium content and the growth time for interlayer were varied. The InGaN interlayer and InN epilayers were grown using N_2 carrier gas. Before the growth of the InGaN layer, a 1 μm thick undoped GaN buffer layer was grown at 1040 °C using a standard two-step process. Two samples were grown on $In_xGa_{1-x}N$ with fixed In contents $x = 0.13$ ($T_g = 720$ °C) and $x = 0.25$ ($T_g = 660$ °C), respectively, and the thickness was ~15–20 nm. Another set of two samples were grown with graded indium composition in the interlayer varying from $x = 0$ to 1 by varying TMIn/TMGa ratio and by ramping the temperature. The growth time for these two graded InGaN layers were 660 and 1620 s. These samples however are not discussed in detail as the X-ray data from those samples were not conclusive and the simulation of the X-ray data had not been possible. Table 1 shows details of the samples investigated.

The structural characterization of the InN layers was carried out using a Panalytical X'PERT HRXRD system using CuKα_1 X-rays obtained from a Hybrid 4× monochromator with an angular divergence of ~20 arcs in the scattering plane. A Xenon filled proportional counter was used as the detector. The 2θ axis was collimated by using a 1/2° slit instead of the usual triple axis attachment. This was done so that reasonable intensity could be obtained for all the reflections. Symmetric $\omega/2\theta$ and ω scans for the (0002), (0004), (0006), and ω scans in the skew-symmetric geometry for (10–15), (10–14), (10–13), (10–12), (10–11), and (30–32) reflections were recorded. The mosaicity parameters of the InN layer were extracted from Williamson–Hall (W–H) plot analysis for a set of symmetric reflections like (0002), (0004), and (0006) and we have extracted the value of tilt angle from the slope [14]. The value of twist angle was estimated by recording a series of ω scans in the skew-symmetric geometry, plotting their widths as a function of angle ψ (ψ is the angle between the plane and the sample surface) and fitting the data using the model of tilt and twist as proposed by Srikant et.al [15]. For wurtzite III-nitrides, screw-type dislocations with a Burgers vector $\boldsymbol{b} = <0001>$ result in a tilt of lattice planes. The other type of dislocation in III-nitrides are of edge type with a Burgers vector $\boldsymbol{b} = 1/3<11\text{–}20>$. For a random distribution of dislocations, the dislocation density (N) can be related to the tilt/twist and the respective Burgers vector $\boldsymbol{b}$ by the expression: $N = \alpha^2/4.35\boldsymbol{b}^2$ where, α is the value of the tilt/twist and $\boldsymbol{b}$ is the corresponding Burgers vector's magnitude [16].

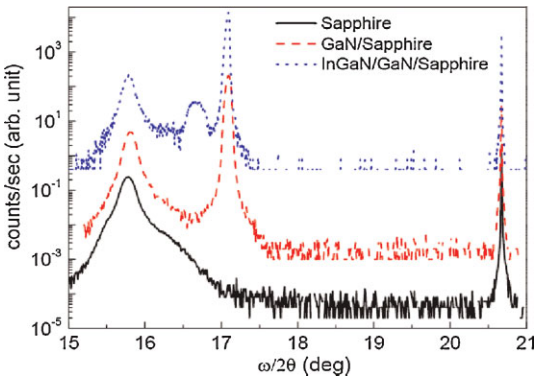

Figure 1 (online color at: www.pss-a.com) Typical (0002) $\omega/2\theta$ XRD rocking curves of InN films grown directly on a sapphire substrate, on a GaN buffer layer, and on an $In_{0.13}Ga_{0.87}N$ intermediate layer between GaN buffer and InN film. Scans are vertically displaced for clarity.

Room/low temperature PL measured using a 0.67 m monochromator and Ar^+ ion laser excitation and Hall measurements in the van-der-Pauw geometry were used to determine the carrier concentration and mobility. A Digital Instruments Nanoscope III atomic force microscope (AFM) operated in contact mode was used to record the surface morphology of the samples.

3 Results and discussion Figure 1 compares the (0002) X-ray rocking curve in $\omega/2\theta$ geometry from 0.2 μm thick InN epilayers deposited under the same growth

Table 1 Details of samples studied.

sample no.	V/III ratio	underlying layer	FWHM of (0002) ω scan (°)	carrier concentration (cm^{-3})	mobility (cm^2/Vs)	absorption edge (eV)
TS06033	18,700	sapphire	0.82	2.51×10^{19}	132	1.04
TS06009	18,700	GaN	0.67	2.41×10^{19}	124	1.1
TS06011	18,700	$In_xGa_{1-x}N$	0.79	1.72×10^{19}	191	1.05
TS06014	18,700	$In_{0.13}Ga_{0.87}N$	0.76	2.08×10^{19}	117	1.05
TS06034	18,700	$In_xGa_{1-x}N$	0.98	1.90×10^{19}	149	1.03
TS06035	18,700	$In_{0.25}Ga_{0.75}N$	0.74	1.52×10^{19}	157	1.01

All samples were grown at $T_g = 530$ °C and reactor pressure of 500 Torr.

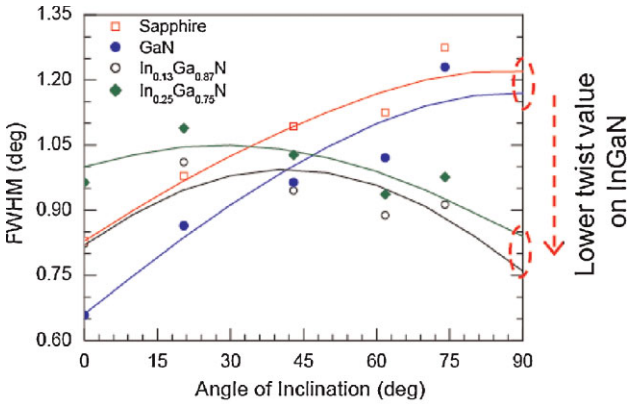

Figure 2 (online color at: www.pss-a.com) The FWHM of various reflections for InN films deposited on different buffer layers as a function of inclination angle. Solid lines are the fit obtained by using the model of Srikant et al.

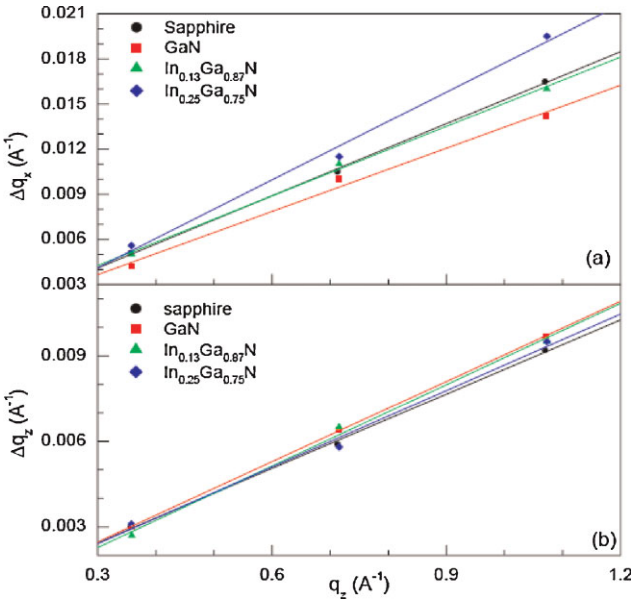

Figure 3 (online color at: www.pss-a.com) Broadening in the reciprocal space as obtained from symmetric scans (a) along ω axis (q_x) and (b) along the $\omega/2\theta$ axis (q_z) measured for the (0002), (0004), and (0006) reflections.

conditions directly on sapphire, on a GaN buffer layer and with an $In_{0.13}Ga_{0.87}N$ interlayer. A close observation reveals similar values of the peak positions and the FWHM for the InN layer. Low temperature PL and room temperature absorption measurements indicated that the bandgap values are all very similar. Though the mobility value for the sample with InGaN interlayer was slightly higher, no remarkable difference in the carrier concentration ($\sim 1 \times 10^{19}\,cm^{-3}$) was observed for different buffer layers.

Figure 2 summarizes the measured FWHM (points) of various skew-symmetric reflections for InN layers and the model fit (solid lines) which are plotted as a function of the angle of inclination. The vertical axis on the left-hand side indicates the value of tilt, the value of twist is determined by extrapolating the fit to $\psi = 90^\circ$, which is shown on the right hand side. It is found that by inserting an InGaN interlayer the angle of twist is reduced, albeit at a small increase in the angle of tilt. The lowest value of edge dislocation density measured from the twist value is $4 \times 10^9\,cm^{-2}$. The reduction in twist is remarkable as our earlier study had found the twist angle was relatively insensitive to growth conditions, and was reduced only on growing thicker layers [4]. Growth on an InGaN interlayer hence offers a route to a reduced edge dislocation density for a given layer thickness. We surmise that the reduction in twist and hence the edge dislocation density is related to the difference in the size of islands during the initial nucleation of the InN layer on the InGaN layer. Since the strain difference is reduced, there is a greater propensity for larger islands to be formed. Further, the evolution of defects in the InGaN interlayer (which is under compressive stress) may influence the edge dislocation in the InN layer. To probe the island sizes/lateral coherence lengths, and to also get a better estimate on the values of tilt, W–H plots for these samples (Fig. 3a and b) were analyzed. The slope of the lines in Fig. 3a confirms the observation that tilt value of samples grown on the InGaN interlayers are slightly higher than those on the GaN buffer. InN layers deposited directly on sapphire also have a higher value of tilt. Figure 3b shows the broadening of the reciprocal lattice points along the q_z direction which represents the microstrain in the epilayer. The slopes are nearly identical, signifying that different buffer layers have a marginal effect if any on the microstrain. However the lateral coherence lengths in all cases turn out to be larger than what can be reliably probed by X-ray diffraction measurements, thus the W–H plots cannot provide a quantitative estimate of this.

Another route to estimate the island sizes during nucleation of the InN layer would be from surface morphology measurements via AFM. The sizes of the islands seen on the surface after the growth of the layer should be related, to first order, to the sizes of the initial islands. Though we have looked at the surface morphology of various InN samples with AFM, a quantitative comparison of island sizes based on AFM images is difficult, given the limited data available. While AFM images are relatively easy to analyze for height differences, lateral dimensions measured from AFM are dependent on the nature of the tip-sample interaction. In cases where the differences between samples are small, it would require evaluation of averages over a large number of samples taken under similar conditions for meaningful comparisons to be made.

4 Conclusions We have performed a detailed microstructural analysis of MOVPE grown InN layers deposited directly on sapphire, on GaN buffer and on InGaN interlayers between GaN and InN films. Analysis of X-ray diffraction data shows that twist angle and hence the density of edge

dislocations is reduced by inserting an $In_xGa_{1-x}N$ interlayer. Though growth on an InGaN interlayer provides an interesting route to improve material quality, further comprehensive analysis is needed to clarify the mechanism of reduction in defect density.

References

[1] A. G. Bhuiyan, A. Hashimoto, and A. Yamamoto, J. Appl. Phys. **94**, 2779 (2003).
[2] A. Kadir, T. Ganguli, M. R. Gokhale, A. P. Shah, S. S. Chandvankar, B. M. Arora, and A. Bhattacharya, J. Cryst. Growth **298**, 403 (2007).
[3] A. Kadir, T. Ganguli, R. Kumar, M. R. Gokhale, A. P. Shah, S. Ghosh, B. M. Arora, and A. Bhattacharya, Appl. Phys. Lett. **91**, 111913 (2007).
[4] T. Ganguli, A. Kadir, M. R. Gokhale, R. Kumar, A. P. Shah, B. M. Arora, and A. Bhattacharya, J. Cryst. Growth **310**, 4942 (2008).
[5] Y. Nanishi, Y. Saito, and T. Yamaguchi, Jpn. J. Appl. Phys. **42**, 2549 (2003).
[6] F. K. LeGoues, B. S. Meyerson, J. F. Morar, and P. D. Kirchner, J. Appl. Phys. **71**, 4230 (1992).
[7] D. Schlenker, T. Miyamoto, Z. Chen, F. Koyama, and K. Iga, IEEE Photon Tech. Lett. **11**, 946 (1999).
[8] Y. Takano, M. Hisaka, N. Fujii, K. Suzuki, K. Kuwahara, and S. Fuke, Appl. Phys. Lett. **73**, 2917 (1998).
[9] T. A. Lafford, P. J. Parbrook, and B. K. Tanner, Appl. Phys. Lett. **83**, 5434 (2003).
[10] S. Che, W. Terashima, Y. Ishitani, A. Yoshikawa, T. Matsuda, H. Ishii, and S. Yoshida, Appl. Phys. Lett. **86**, 261903 (2005).
[11] T. Ohashi, P. Holmstrom, A. Kikuchi, and K. Kishino, Appl. Phys. Lett. **89**, 041907 (2006).
[12] S. Che, T. Mizuno, X. Wang, Y. Ishitani, and A. Yoshikawa, J. Appl. Phys. **102**, 083539 (2007).
[13] H. Hartono, P. Chen, S. J. Chua, and E. A. Fitzgerald, Thin Solid Films **515**, 4408 (2007).
[14] M. E. Vickers, M. J. Kappers, R. Datta, C. McAleese, T. M. Smeeton, F. D. G. Rayment, and C. J. Humphreys, J. Phys. D **38**, A99 (2005).
[15] V. Srikant, J. S. Speck, and D. R. Clarke, J. Appl. Phys. **82**, 4286 (1997).
[16] C. G. Dunn and E. F. Koch, Acta Metall. **5**, 548 (1957).